Resonant magnetoabsorption of millimeter-wave radiation in the quasi-two-dimensional organic metals α-(BEDT-TTF)$_2M$Hg(SCN)$_4$ (M=K,Tl)

S. V. Demishev, A. V. Semeno, N. E. Sluchanko, N. A. Samarin, I. B. Voskoboinikov, and V. V. Glushkov
General Physics Institute of Russian Academy of Sciences, Vavilov Street, 38, 117942 Moscow, Russia

J. Singleton, S. J. Blundell, S. O. Hill, and W. Hayes
The Clarendon Laboratory, University of Oxford, Parks Road, Oxford OX1 3PU, United Kingdom

M. V. Kartsovnik and A. E. Kovalev
Institute of Solid State Physics of Russian Academy of Sciences, 142432 Chernogolovka, Russia

M. Kurmoo and P. Day
Royal Institution, 21 Albemarle Street, London W1X 4BS, United Kingdom

N. D. Kushch
Institute of the Chemical Physics of Russian Academy of Sciences, 142432 Chernogolovka, Russia
(Received 10 November 1995; revised manuscript received 12 February 1996)

The magnetoabsorption of millimeter-wave radiation by single crystals of the organic metals α-(BEDT-TTF)$_2$TlHg(SCN)$_4$ and α-(BEDT-TTF)$_2$KHg(SCN)$_4$ has been studied in the frequency range 30–120 GHz. The experiments reveal two dominant contributions to the magnetoabsorption spectra. The first is interpreted as the cyclotron resonance of two-dimensional carriers, and is characterized by broad lines (linewidth/magnetic field $\Delta B/B\sim 0.5-1$). In addition to a resonance exhibiting a cyclotron mass $m_c\sim 2.8m_0$, there are two further lines corresponding to frequency-dependent cyclotron masses in the ranges $m_c\sim(1-1.5)m_0$ and $m_c\sim(0.5-0.8)m_0$. This frequency dependence is believed to result from many-body effects. The second contribution to the magnetoabsorption is formed by a series of narrow lines with $\Delta B/B\sim 0.03-0.1$ and amplitudes 5–10 times smaller than the features interpreted as cyclotron resonances. These narrow lines are attributed to a superposition of modes due to antiferromagnetic resonance and conduction-electron-spin resonance (ESR). The feature characteristic of antiferromagnetic resonance is the presence of a mode with a frequency that decreases with increasing magnetic field. The magnetoabsorption structure attributed to ESR consists of a relatively broad maximum upon which a sharp dip is superimposed. This behavior is believed to be analogous to the resonant transparency observed in thin metallic films undergoing ESR. [S0163-1829(96)01420-0]

I. INTRODUCTION

During the last decade, the physics of quasi-one-dimensional (Q1D) and quasi-two-dimensional (Q2D) organic conductors has generated great interest, as witnessed by the large number of magnetotransport studies of such materials (see, e.g., Ref. 1 and references therein). However, experimental (e.g., Refs. 2–15) and theoretical[16] studies of the absorption of millimeter-wave radiation by organic conductors have been relatively sparse, in spite of the very valuable complementary information that they can potentially yield. In addition to straightforward electron-spin-resonance (ESR) experiments,[4,5] features attributed to antiferromagnetic resonance (AFMR),[2,3,10,11] cyclotron resonance (CR),[6–11,14,15] and spin-density-wave (SDW) excitations[15] have been reported. However, the accounts of suggested CR are at first sight both complex and, to a certain extent, contradictory.

Most of the reports of apparent CR in organic metals involve charge-transfer salts of the ion BEDT-TTF [bis(ethylenedithio)tetrathiofulvalene], and in particular the family α-(BEDT-TTF)$_2M$Hg(SCN)$_4$, where M=K,Tl,NH$_4$.[6–11] The electrical conductivity of the latter systems has a well-defined Q2D character, and their calculated Fermi surfaces (based on room-temperature crystallography data) consist of a closed Q2D pocket and a Q1D open section.[17] Moreover, the variation of the anion component M changes the low-temperature ground state from superconducting ($T_c\approx 1$ K; M=NH$_4$) to an antiferromagnetic metallic state attributed to the presence of a SDW ($T_N\sim 8-10$ K; M=K,Tl,Rb) (see Refs. 18–23 and references therein). The observation of magneto-optical features attributed to CR was first reported in Ref. 6 for the case of α-(BEDT-TTF)$_2$KHg(SCN)$_4$. Two lines, with linewidths $\Delta B\sim 1-2$ T and a resonant frequency proportional to magnetic field B, were observed in the frequency range $\nu=\omega/2\pi=316-698$ GHz. The positions of these features corresponded to cyclotron masses $m_{c1}\sim m_0$ and $m_{c2}\sim 0.4m_0$, where m_0 is the free-electron mass.[6] Using the standard formula for the complex conductivity $\sigma(\omega,B)$ of charge carriers in a magnetic field,[24] the linewidths at $B\sim 10$ T (Ref. 6) yielded $(\omega_{c1}\tau_1)\sim 10-15$ and $(\omega_{c2}\tau_2)\sim 7$ (here ω_c is the cyclotron frequency eB/m_c, and τ is the relaxation time). Further results were subsequently obtained for other BEDT-TTF charge-transfer salts;[7–11] e.g., in the

case of α-(BEDT-TTF)$_2$NH$_4$Hg(SCN)$_4$ at frequencies ν=45–65 GHz (i.e., much lower frequencies than those of Ref. 6), a resonance corresponding to a cyclotron mass $m \sim m_0$, and with $(\omega_c \tau) \sim 5$ was observed.[7]

However, the interpretation of these features in the millimeter-wave magnetoabsorption of BEDT-TTF salts as CR (Refs. 6–9) is not without problems. For instance, the BEDT-TTF salts studied possess effective masses derived from Shubnikov–de Haas and de Haas–van Alphen measurements which lie in the range $m^* \sim (1.4$–$3.5) m_0$[6–9,18–22,25] whereas the magneto-optical features interpreted as CR yield cyclotron masses $m_c \sim m_0$.[6–9] This difference has been attributed[6–9] to electron-electron interactions, with the mass deduced from CR being identified as the dynamical mass (i.e., renormalized only by electron-phonon interactions) and that derived from Shubnikov–de Haas and de Haas–van Alphen measurements identified as the effective mass (i.e., renormalized by both electron-electron and electron-phonon interactions). Furthermore, typical Dingle temperatures of the BEDT-TTF salts studied[18–22,25] imply $(\omega_c \tau) \sim 1$ at ν=100 GHz; the lines interpreted as CR in Refs. 6–9 are therefore a factor $\sim$2–5 narrower than expected. However, differences between Dingle and CR scattering rates of this size are by no means without precedent in 2D systems (the Dingle temperature may contain the effects of inhomogeneities, whereas CR is a ''local'' probe of the Landau-level spacing[26,27]), and it might be argued[6] that the relative narrowness of the CR lines could also result from the smaller value of m_c compared to m^*.

In subsequent studies of α-(BEDT-TTF)$_2$KHg(SCN)$_4$,[10,11] an additional broad feature with the attributes of Q2D CR was observed with an apparent cyclotron mass $m_c \sim 2.8 m_0$ (i.e., larger than the values $m^* \sim 1.4$–$2.0 m_0$ derived from the most prominent series of Shubnikov–de Haas oscillations observed in this material[18–22]), and a relaxation time such that $(\omega_c \tau) \sim 2$. In the same studies, several very sharp magnetoabsorption features were also noted ($\Delta B \sim 0.1$ T) at frequencies $<$120 GHz. These were attributed to ESR and AFMR rather than CR,[10,11] because their positions did not depend on the magnetic-field orientation in the manner expected for Q2D CR; some were excited even when the magnetic field was parallel to the conducting plane (i.e., no 2D quantization of orbital motion possible). Some of these narrow lines[10,11] lay close to the extrapolated low-frequency positions of the two apparent CR with $m_c \sim m_0$ and $m_c \sim 0.4 m_0$ reported in Ref. 6 for frequencies $\gtrsim$300 GHz. The assignment of these features as CR in Ref. 6 was thus called into question.[10,11]

In order to try to reconcile the results of the various magneto-optical experiments referred to above, we have carried out a careful study of the resonant magnetoabsorption of single crystals of α-(BEDT-TTF)$_2$$M$Hg(SCN)$_4$ (M=K,Tl) in the frequency range ν<150 GHz. Great care has been taken to distinguish between features due to ESR, AFMR, and CR, using various criteria such as characteristic linewidth and its temperature dependence and the variation of resonance position with magnetic-field orientation. The results show a satisfactory agreement with the early high-frequency studies,[6] and indicate several interesting features which seem to be peculiar to organic molecular metals.

II. EXPERIMENTAL DETAILS

Single crystals of α-(BEDT-TTF)$_2$KHg(SCN)$_4$ and its isostructural analog α-(BEDT-TTF)$_2$TlHg(SCN)$_4$ were prepared using standard electrochemical methods.[28] Both salts are known to be in similar metallic antiferromagnetic ground states for magnetic fields less than $\sim$20 T at all of the sample temperatures used in this study (see Refs. 18–23 and references therein). Furthermore, there is strong evidence that both salts possess similar reorganized Fermi surfaces in this low-temperature, low-field state.[20,22] In the present study the millimeter-wave response of the samples was measured at temperatures T=4.2 and 1.8 K in magnetic fields of up to 7 T (i.e., always within the antiferromagnetic phase[18–23]).

One of the primary aims of this work was to make magneto-optical measurements on single crystals of the BEDT-TTF salts with characteristic sizes $2 \times 2 \times 0.3$ mm^3, rather than on the mosaics of several crystals used in previous experiments.[6–9,14,15] The most highly developed millimeter-wave technique for studying small samples involves the use of rectangular or cylindrical resonant cavities.[12,13] An obvious advantage of such an experiment is the fixed geometry of the oscillating electromagnetic fields; in certain very simple cases the sample's conductivity and/or permittivity tensors may be calculated from the response of the loaded cavity.[12,13] However, it will become obvious below that the most important requirement in the identification of the various magneto-optical features observed in BEDT-TTF salts is the ability to make measurements over a wide range of closely spaced frequencies; this rules out the use of the cavity perturbation technique. Quasioptical experiments based on tunable sources such as backward-wave oscillators (BWO's) do possess almost continuous tunability over a wide frequency range;[29] however, such experiments require rather large ($>5 \times 5$ mm^2) transparent samples.

Thus both of the well-established millimeter-wave spectroscopic techniques possesses disadvantages in the case of small, metallic single-crystal BEDT-TTF salt samples. Instead an alternative nonresonant measurement based on tunable BWO's was designed, in which the millimeter-wave radiation is detected by a miniature carbon bolometer of a comparable size to the BEDT-TTF salt single crystals. The sample under study is fixed to the surface of the bolometer using a thin layer of heat-conducting Apiezon grease. Millimeter-wave radiation with a frequency in the range 30–120 GHz is conveyed from a BWO into the cryostat using standard 8-mm rectangular waveguides and then focused onto the sample/bolometer combination using a beam concentrator (a focusing cone of rectangular cross section). The loaded bolometer was mounted on a sapphire rod in good thermal contact with a bath of liquid helium. Steady temperatures for the sample and bolometer were ensured by using a temperature sensor connected to an electronic stabilization circuit which could be used to drive a small heater on the rod. In addition, the sample could be maintained in vacuum or helium exchange gas. The waveguide system was placed in a 7-T vertical-axis superconductive magnet. Two experimental geometries were used. In one case the Poynting vector of the millimeter waves and the applied magnetic field were both perpendicular to the Q2D conducting planes of the samples. In the second case the magnetic field and the Poyn-

ting vector were also parallel, but tilted by an angle θ to the normal to the conducting plane of the samples.[30]

The nonresonant method adopted allows a wide range of frequencies to be used, but sacrifices the opportunity of obtaining detailed information about the electrodynamical response of the sample, as the oscillating electromagnetic fields around the sample are not of a well-defined geometry. In our qualitative interpretation of the data we have used the analytical approximations derived below as Eqs. (1)–(3), the validity of which has been tested by measuring samples with a well-known millimeter-wave response.

It is assumed that the signal from the bolometer is proportional to the absorbed power P in what we shall refer to as the measuring unit, i.e., the cone, bolometer and sample combination. As no millimeter-wave radiation leaves the system, P may be expressed in terms of the complex reflection coefficient Γ (i.e., the losses in the waveguide are neglected),[31]

$$P = P_0(1-|\Gamma|), \tag{1}$$

$$\Gamma = (Z_u - Z_c)/(Z_u + Z_c), \tag{1a}$$

where Z_c and Z_u are the impedances of the waveguide and the measuring unit, respectively. Z_u includes the impedances of the bolometer and the cone and the sample impedance Z_σ. We assume that the sample and the other impedances act as though they are in parallel, so that

$$Z_u^{-1} = Z_0^{-1} + Z_\sigma^{-1}, \tag{2}$$

where Z_0 is the impedance of the empty measuring unit. In the present apparatus it is known that $\mathrm{Re}\, Z_0 \gg \mathrm{Im}\, Z_0$, so that Z_0 can be considered to be real. Substituting (2) into Eq. (1), and retaining only the terms linear in the sample conductivity (i.e., in Z_σ^{-1}), we obtain

$$P = P_1 + P_2, \tag{3a}$$

$$P_1 \approx P_0(1-|\Gamma_0|), \tag{3b}$$

$$P_2 \approx 2P_0|\Gamma_0| f(Z_c/Z_0)\,\mathrm{Re}(Z_c/Z_\sigma), \tag{3c}$$

$$f(x) \approx (2+x)/(1-x^2), \quad x = Z_c/Z_0, \tag{3d}$$

where P_0 is the incident power, P_1 is the power absorbed in the empty measuring unit (i.e., with no sample), and $\Gamma_0 = (Z_0 - Z_c)/(Z_0 + Z_c)$ is its reflection coefficient. The function P_2 gives additional absorption due to the sample, and $f(Z_c/Z_0)$ describes the change in absorption which takes place when the sample is placed in the measuring unit.

The exact form of the function $f(x)$ [Eq. (3d)] can be obtained only in very simplified models.[31] In the present experiments $Z_c < Z_0$, so that the insertion of the sample into the measuring unit will lead to additional absorption because $f(Z_c/Z_0) > 0$. In the interpretation of resonant features in the magnetoabsorption $P(B)$, it is important that $f(x)$ is smooth over the range of conditions covered in the experiment, and that it increases monotonically with x. Several trial experiments were carried out with test samples exhibiting well-characterized resonant and nonresonant behaviors (e.g., DPPH, films of conventional metals, doped semiconductors, etc.), which indicate that $f(x)$ does indeed behave in this manner.

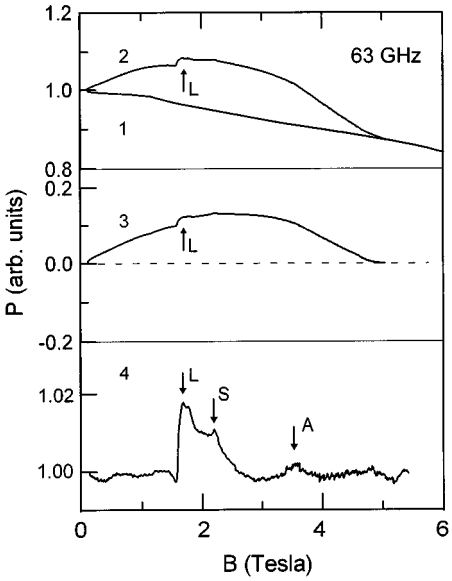

FIG. 1. Magnetoabsorption of α-(BEDT-TTF)$_2$TlHg(SCN)$_4$ at ν=63 GHz; Curve 1: empty measuring unit: Curve 2: measuring unit loaded with sample. Curve 3: function $P_2(B)$ showing the broad peak due to absorption by 2D carriers (i.e., curve 2−curve 1). Curve 4: function $P_2(B)/\tilde{P}_2(B)$ showing magnetic resonances (marked by arrows). Curves 1 and 2 are in units of $P(B)/P(0)$, and the temperature is 1.8 K. See Eqs. (1)–(3) and subsequent discussion for definitions of the various P functions.

In spite of the approximations used in their derivation, Eqs. (1)–(3) appear to reproduce the behavior of the apparatus when it is loaded with single-crystal samples of BEDT-TTF salts, and form the basis of a qualitative understanding of all of the data in this paper. Typical experimental results are shown in Fig. 1, which displays absorbed power P versus magnetic field for α-(BEDT-TTF)$_2$TlHg(SCN)$_4$ at a constant frequency. When the sample is inserted into the measuring unit, an additional broad feature in the magnetoabsorption appears (compare curves 1 and 2 in Fig. 1) on the smooth background. Note that this background dependence on B corresponds to the changing $P_1(B)$ due to a variation of Z_0 caused by the magnetoresistance of the bolometer; it is practically linear in B. Furthermore, the functions $R(Z_c/Z_0)$ and $f(Z_c/Z_0)$ are smooth and well behaved. Therefore, any nonmonotonic variation of $P(B)$ (Fig. 1, curve 2) is due to features in $P_2(B)$ associated with the insertion of the organic metal sample (Fig. 1, curve 3). Simple calculations show that the structure in $P_2(B)$ cannot be due to features in the dc magnetoresistance of the samples; for $B < 7$ T both α-(BEDT-TTF)$_2$KHg(SCN)$_4$ and α-(BEDT-TTF)$_2$TlHg(SCN)$_4$ possess a monotonically increasing magnetoresistance which has no sharp field-dependent features save very small Shubnikov–de Haas oscillations.[18–22]

Several narrower lines of smaller amplitude may be perceived superimposed on the broad features in $P_2(B)$ (see the arrows in Fig. 1). In order to better distinguish between broad and narrow features, $P_2(B)$ was coarsely smoothed to

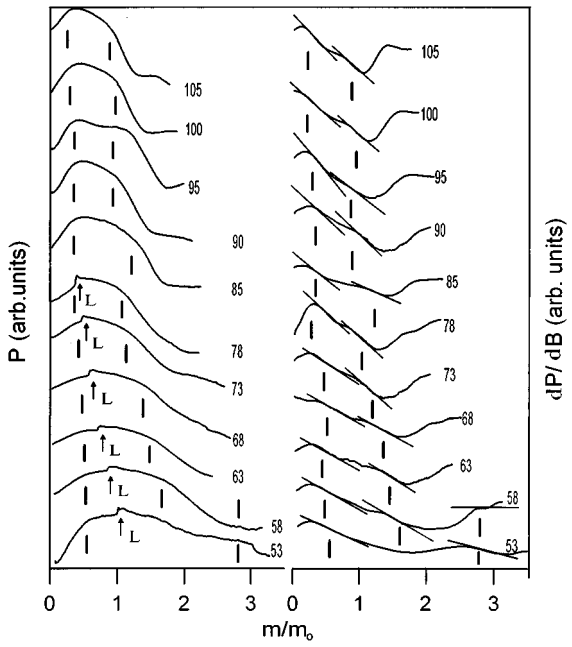

FIG. 2. The functions $P(B)$ (left-hand curves) and dP/dB (right hand curves) at various frequencies and $T=1.8$ K for α-(BEDT-TTF)$_2$TlHg(SCN)$_4$. The horizontal axis represents the magnetic field in units of the free-electron mass (see text). Dashes mark the cyclotron resonance lines and arrows mark magnetic resonances. Points of inflection (see text) are indicated on the right-hand curves using tilted lines. The numbers near the curves correspond to the frequency in GHz.

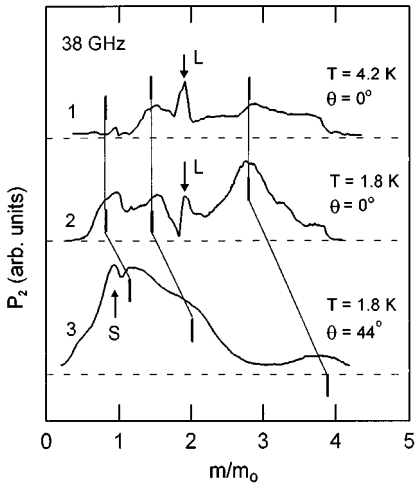

FIG. 3. The influence of temperature and sample tilt on the $P_2(B)$ function for α-(BEDT-TTF)$_2$KHg(SCN)$_4$ at $\nu=38$ GHz. The temperatures are curve 1, 4.2 K; curve 2, 1.8 K; and curve 3, 1.8 K. Curves 1 and 2 correspond to the case when the magnetic field is perpendicular to the sample 2D conducting planes ($\theta=0°$). The positions of the cyclotron resonances are marked by dashes, and magnetic resonances are marked by arrows. Curve 3 was obtained for a magnetic field tilted by $\theta=44°$ from the normal to the sample 2D conducting planes. The cyclotron resonance markers above curve 3 are obtained by extrapolating the $\theta=0°$ positions using Eq. (4).

yield $\tilde{P}_2(B)$, and then the ratio $P_2(B)/\tilde{P}_2(B)$ was calculated. An example of this procedure is shown as curve 4 in Fig. 1; three sharp lines which have been labeled L, S, and A can be distinguished. The relatively good signal-to-noise ratio of the equipment is demonstrated by the systematic detection of feature A, corresponding to some 0.3–0.4 % of $P_2(B)$, at several frequencies.

Following the discussions of linewidth in Sec. I, the broad features in $P(B)$, which have amplitudes $\sim$10%, are tentatively identified as CR-like excitations of the Q2D carriers.[30] Similarly, the narrow lines with amplitudes $\leqslant$2% are tentatively ascribed to magnetic resonance (i.e., ESR and AFMR). The next sections describe the characteristics of the resonant magnetoabsorption in more detail, and give additional arguments which strongly support this interpretation.

III. ABSORPTION OF MICROWAVE RADIATION BY FREE-CHARGE CARRIERS

A. General features

In the identification of the various resonances, it is instructive to analyze the evolution of the shape of the $P(B)$ curves with millimeter-wave frequency. As an example of this, data from α-(BEDT-TTF)$_2$TlHg(SCN)$_4$ at $T=1.8$ K are shown in Fig. 2, left-hand side; the α-(BEDT-TTF)$_2$KHg(SCN)$_4$ data were qualitatively very similar. In order to facilitate comparison, the $P(B)$ data in Fig. 2 are plotted against a magnetic-field scale in the units $eB/2\pi\nu m_0$; a cyclotron resonance representing a constant cyclotron mass would therefore appear at a fixed position corresponding to that mass in units of m_0.

The shapes of the curves in the left-hand part of Fig. 2 seem to indicate that the broad feature in $P(B)$ consists of a superposition of two wide maxima which become better resolved in the region $\nu\sim$100 GHz. In view of the sloping background behavior of $P_1(B)$ (see Sec. II), the true positions of the maxima are extracted as follows. First the experimental $P(B)$ curves are smoothed to remove the narrow magnetic resonances seen in Fig. 1, curve 4, and then their derivatives dP/dB are calculated. Maxima in absorption then correspond to the inflection points of the dP/dB curves. The results of this procedure are shown on the right-hand side of Fig. 2, with the positions of the maxima marked by vertical dashes.

In the whole frequency range under investigation, two features around $m_c\sim 0.5m_0$ and $m_c\sim(1-1.5)m_0$ with frequency-dependent positions, are observed (Fig. 2). In addition, for frequencies $<$60 GHz, a weaker resonance with $m_c\sim 2.8m_0$ is seen (Fig. 2).

Very similar features are observed in the millimeter-wave magnetoabsorption of α-(BEDT-TTF)$_2$KHg(SCN)$_4$. Figure 3 shows that, once again, three broad maxima are observed, in this case corresponding to cyclotron masses $m_c\sim 0.8m_0$, $m_c\sim 1.4m_0$, and $m_c\sim 2.8m_0$ (Fig. 3, curves 1 and 2). Figure 3 also shows the characteristic effects of temperature variation and tilting the magnetic field on these broad features. For α-(BEDT-TTF)$_2$KHg(SCN)$_4$ at $T=4.2$ K, the most prominent feature is the resonance with $m_c\sim 1.4m_0$. Lowering the temperature to $T=1.8$ K leads to an increase in the sharpness of this resonance. However, the most dramatic changes on lowering the temperature are the substantial increases in amplitude of the resonances with $m_c\sim 0.8m_0$ and $m_c\sim 2.8m_0$ (cf. curves 1 and 2 of Fig. 3). The latter feature then has the largest relative amplitude of all of the magneto-

optical features, and its frequency dependence is similar to that of the corresponding resonance with $m_c \sim 2.8m_0$ in α-(BEDT-TTF)$_2$TlHg(SCN)$_4$, which is observed as a broad maximum of the $P(B)$ at $\nu \leqslant 53$ GHz (Figs. 2 and 3) and becomes narrower at $\nu = 58$ GHz (Fig. 2). At higher frequencies this feature moves outside the magnetic-field range available in the present apparatus.

If the external magnetic field is inclined at an angle θ to the normal to the Q2D conducting plane, all three of the broader resonances shift to higher magnetic fields, or, on the renormalized field scale, to higher effective masses (Fig. 3, curve 3). Within experimental errors,[30] the masses observed followed the simple relationship

$$m_c(\theta) = m_{c0}/\cos(\theta) \tag{4}$$

at all tilt angles. This behavior is characteristic of 2D Landau quantization, dependent only on the normal component of magnetic field.[24] In Fig. 3, the vertical dashes near curve 3 for $\theta = 44°$ mark the calculated resonance positions derived from Eq. (4) and the $\theta = 0$ resonance fields.

The temperature and tilt angle dependences of the broad magnetoabsorption features in α-(BEDT-TTF)$_2$TlHg(SCN)$_4$ and α-(BEDT-TTF)$_2$KHg(SCN)$_4$ both strongly support their identification as CR. The variation of the amplitude of the resonances with temperature (Fig. 3) probably reflects the temperature dependence of the relaxation time τ due to the thermal excitation of low-energy phonons. In contrast, the widths of the narrow features tentatively attributed to magnetic resonance show little temperature dependence between 1.8 and 4.2 K; magnetic dipole transitions such as ESR are generally less strongly coupled to lattice vibrations than are electric dipole transitions such as CR.[30]

The physical picture of CR in charge-transfer salts is likely to be rather different from that in a conventional metal. In the latter case, carriers move in an inhomogeneous oscillating electric field E.[30,32] However, in contrast, the large skin depth δ in organic metals (the skin depth of the α-phase BEDT-TTF salts is estimated to be $\delta \sim 20$ μm from conductivity data,[33] considerably larger than skin depths of conventional metals) and the experimental geometry used in this work (Sec. II) imply that for each Q2D conducting plane $E = \text{const}$, and that no movement of carriers through an electric field gradient takes place. Nevertheless, the magnitude of the electric field will decrease with increasing distance from the surface (see Fig. 4, inset, which schematically represents the experimental geometry for CR in organic metals).

In order to discuss this point further, let the z axis be parallel to the normal to the sample surface (i.e., perpendicular to the Q2D planes); assuming that z increases into the sample we can write $E(z) = E(0)\exp(-z/\delta)$. As the electric field is constant in each Q2D conducting plane, the connection between current density and electric field becomes local, i.e., $j(z) = \sigma E(z)$. Under these conditions the expression for the sample impedance becomes

$$Z_\sigma = \frac{E(0)}{\int_0^d j(z)dz} \approx (\sigma\delta)^{-1}, \tag{5}$$

where d is the sample thickness; in deriving the expression for Z_σ we have taken into account the condition $d \gg \delta$.

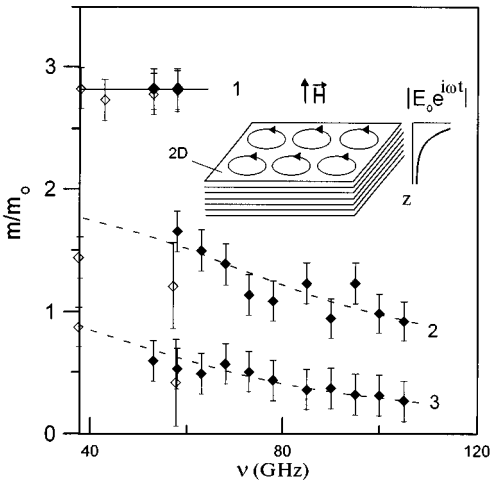

FIG. 4. Experimental cyclotron masses for α-(BEDT-TTF)$_2$TlHg(SCN)$_4$ (black dots) and α-(BEDT-TTF)$_2$KHg(SCN)$_4$ (white dots). The set of points labeled 1 represent the high-field resonance, while 2 and 3 are the frequency-dependent branches corresponding to the most prominent magnetoabsorption peak (see Fig. 2). The curves are guides to the eye, and the error bars are derived from the width of the points of inflection in dP/dB (see Fig. 2). A schematic representation of the experimental geometry is shown in the inset.

Equations (1)–(5) show that $P_2 \sim \text{Re}\,\sigma(\omega,B)$. In consequence, it can be seen that CR in BEDT-TTF salts is rather more closely related to CR in semiconductor systems than to that in conventional metals; in semiconductors, the absorption coefficient is also proportional to $\text{Re}\{\sigma(\omega,B)\}$ (see also the discussion in Ref. 6, where the same point was inferred from the qualitative behavior of the resonances). The experimental form of the function $P(B)$ is in good agreement with this suggestion (Fig. 1).

In such cases, the Drude-Lorentz model can be used to derive the complex conductivity at angular frequency ω and magnetic field B,[24]

$$(\omega,B) = \frac{e^2 n}{m}\,\frac{i(\omega-\omega_c)+1/\tau}{(\omega-\omega_c)^2+(1/\tau)^2}, \tag{6}$$

where $\omega_c = eB/m_c$ is the cyclotron frequency, τ is the relaxation time, and e and n denote the charge and concentration of the carriers, respectively. Consequently, as ω_c becomes $\gg\omega$, $\text{Re}\,\sigma(\omega,B) \to 0$, and so $P_2 \to 0$. Therefore, the additional absorption due to CR will only be large over a limited range of magnetic field, as observed experimentally (see Fig. 1, curves 1 and 2). In summary, all evidence presented thus far therefore strongly suggests that the broad magnetooptical features in $P(B)$ (Figs. 1–3) are due to CR of free Q2D carriers in the charge-transfer salts.

B. Frequency-dependent cyclotron masses

The frequency dependence of the cyclotron masses derived from the positions of the broad features in $P(B)$ for α-(BEDT-TTF)$_2$TlHg(SCN)$_4$ and α-(BEDT-TTF)$_2$KHg(SCN)$_4$ is shown in Fig. 4. In addition to the CR with $m_c \approx 2.8m_0$ (Fig. 4, curve 1), two branches with frequency-dependent $m_c(\omega)$, corresponding to the main features of the absorption (see Fig. 2), are observed (Fig.

4, curves 2 and 3). If the CR in these organic metals were purely a single-particle effect, one might expect a resonance with a frequency-independent cyclotron mass $m_c=(1.4-2.0)m_0$, i.e., identical to the effective mass derived from the most prominent series of Shubnikov–de Haas oscillations in α-(BEDT-TTF)$_2$TlHg(SCN)$_4$ and α-(BEDT-TTF)$_2$KHg(SCN)$_4$.[18–20,22] However, it is known that descriptions within a Drude-Lorentz model of the experimental reflectance spectra of high-T_c superconductors and heavy fermion systems require frequency-dependent carrier masses and relaxation times.[34] This behavior is believed to result from strong Fermi-liquid effects. The data obtained in this work for α-(BEDT-TTF)$_2$TlHg(SCN)$_4$ and α-(BEDT-TTF)$_2$KHg(SCN)$_4$ (Fig. 4) suggest that similar phenomena take place in BEDT-TTF charge-transfer salts. However, it should be noted that in contrast to the results reported in Ref. 34, evidence of frequency-dependent carrier mass in the present work follows from direct measurements of features in $\sigma(\omega,B)$ (Figs. 1–3); i.e., the frequency-dependent masses are calculated from the CR condition $2\pi\nu=eB/m(\omega)$, and not just as fitting parameters in a description of the conductivity.

The data in this work suggest that the generalized Drude-Lorentz model [Eq. (7)] with frequency- and temperature-dependent relaxation times and frequency-dependent effective masses may be sufficient to describe the millimeter-wave magnetoabsorption of BEDT-TTF charge-transfer salts. The possibility of CR with $m_c=m(\omega)$ in organic metals has been previously suggested,[11,35] but we believe that the present data form the first direct evidence for this effect.

The frequency dependence of the two lower cyclotron mass branches (Fig. 4, curves 2 and 3), corresponding to the main broad magnetoabsorption peak (Fig. 2), has two interesting trends. One might expect that in the limit $\omega\rightarrow 0$ one of the $m(\omega)$ branches would tend to the effective mass determined from the Shubnikov–de Haas or de Haas–van Alphen effects. The quantum oscillations observed in the antiferromagnetic phases of α-(BEDT-TTF)$_2$TlHg(SCN)$_4$ and α-(BEDT-TTF)$_2$KHg(SCN)$_4$ are rather complex in form, and the effective masses deduced vary somewhat depending on the method of extraction (see, e.g., Refs. 18–20 and 22); however, the most prominent series of oscillations yields effective masses in the range $1.4-2.0m_0$. Inspection of Fig. 4 reveals that the central branch (curve 2) is indeed tending toward a value in this range as $\omega\rightarrow 0$. In the opposite limit, $\omega\rightarrow\infty$, the two lower branches in Fig. 4 appear to be approaching the values $m_c\sim m_0$ and $m_c\sim 0.4m_0$ observed in the high-frequency studies of Ref. 6. This strongly suggests that the assignment of the magneto-optical features reported in Ref. 6 to CR is correct.

Finally, we must remark that the form of the Fermi surface of the antiferromagnetic states of α-(BEDT-TTF)$_2$TlHg(SCN)$_4$ and α-(BEDT-TTF)$_2$KHg(SCN)$_4$ remains somewhat controversial (see, e.g., Refs. 18–23). It would therefore be premature to attempt to assign the observed CR to particular Fermi-surface pockets. Similarly, in the absence of a reliable Fermi-surface model, one cannot comment on the possibility that Q1D CR,[16] caused by open sections of Fermi surface, might give rise to one of the resonances observed.[35] However, the Fermi-surface models proposed to explain the magnetotransport and de Haas–van Alphen data often consist of one or more small Q2D pockets and also magnetic breakdown orbits of a considerably larger k-space area with very small characteristic breakdown fields.[18–22] It is therefore not unreasonable to expect more than one CR in the magnetoabsorption.

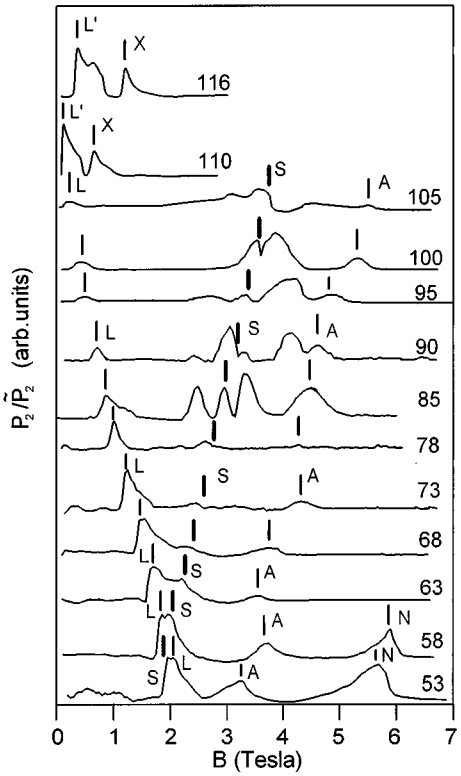

FIG. 5. Magnetic resonances in α-(BEDT-TTF)$_2$TlHg(SCN)$_4$ at $T=1.8$ K. The figures near the curves denote the frequency in GHz. The notation for the resonances is consistent between Figs. 1–3 and 5–7; i.e., the same resonances are marked by the same letters. The magnetic field is perpendicular to the sample Q2D planes.

IV. MAGNETIC RESONANCES

A. General features

In this section we shall consider the narrow lines of relatively small amplitude superimposed on the broad CR features (Fig. 1, curve 4). Typically, this class of resonances possesses half-widths ΔB at half-maximum of $\Delta B/B\sim 0.03-0.1$, whereas for the CR's $\Delta B/B\sim 0.5-1$ (Figs. 1 and 2). According to the literature,[2–4] such narrow lines in the millimeter-wave magnetoabsorption of organic metals can arise from magnetic-resonance phenomena such as AFMR and ESR. Preliminary investigations of α-(BEDT-TTF)$_2$KHg(SCN)$_4$ reported in Ref. 10 appeared to show that up to ten such modes, some very weak, might be present, depending on the frequency and the sample orientation in the field. In the present publication we shall restrict ourselves to describing the stronger lines which can be unambiguously detected at all frequencies when the magnetic field is applied perpendicular to the sample Q2D planes.

Figures 5 and 6 show examples of $P_2(B)/\tilde{P}_2(B)$ (see Sec. II) for α-(BEDT-TTF)$_2$TlHg(SCN)$_4$ and α-(BEDT-TTF)$_2$KHg(SCN)$_4$. In addition to the modes which possess a resonant frequency increasing with magnetic field (lines A

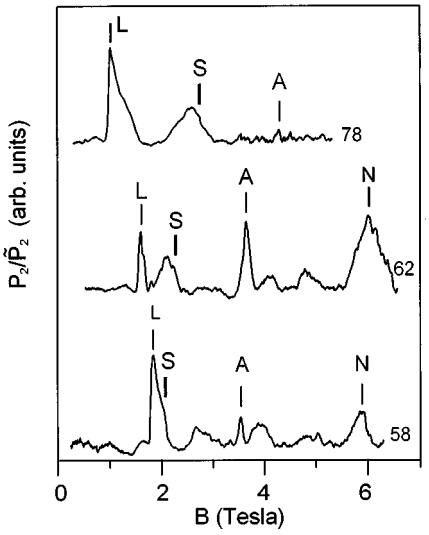

FIG. 6. Magnetic resonances in α-(BEDT-TTF)$_2$KHg(SCN)$_4$ at $T=4.2$ K. The figures near the curves denote the frequency in GHz. The notation for the resonances is consistent between Figs. 1–3 and 5–7, i.e., the same resonances are marked by the same letters. The magnetic field is perpendicular to the sample Q2D planes.

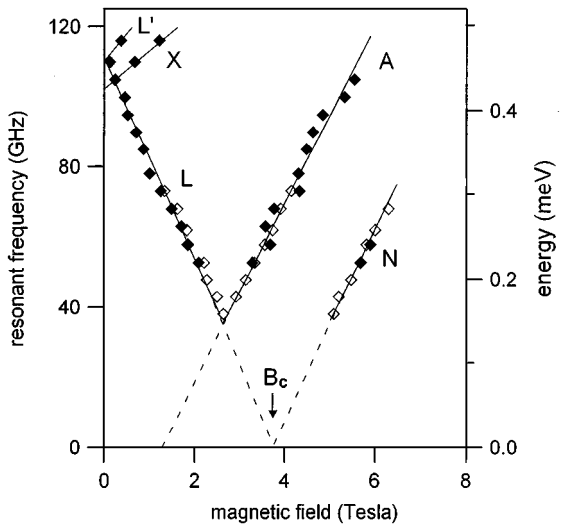

FIG. 7. Positions of the different resonant modes as a function of magnetic field (field applied perpendicular to the sample Q2D planes). Black dots show data for α-(BEDT-TTF)$_2$TlHg(SCN)$_4$, the white dots data for α-(BEDT-TTF)$_2$KHg(SCN)$_4$.

and N), there is a mode (line L) which has a frequency that *decreases* with increasing magnetic field. The shape of line L is rather asymmetric (Figs. 5 and 6), eventually acquiring a characteristic triangular form at higher frequencies. A further resonance (line S) with a complex shape is observed in $P_2(B)/\tilde{P}_2(B)$ close to the expected ESR position at $g\approx 2.01$.[5] Finally, in the frequency range $\nu \gtrsim 110$ GHz, extra lines (L' and X) were found in the magnetoabsorption of α-(BEDT-TTF)$_2$TlHg(SCN)$_4$ (Fig. 5). As will be seen below, lines A, L, L', N, and X appear to have a common origin, and so are discussed together in Sec. IV B. The form of line S is somewhat different from the other modes, and so it will be dealt with separately in Sec. IV C.

B. Possible antiferromagnetic resonance

The frequencies and magnetic fields of the A, L, L', N, and X modes in α-(BEDT-TTF)$_2M$Hg(SCN)$_4$ (M=K, Tl) are shown in Fig. 7. Note that the positions of lines L, A, and N are not, within experimental error, affected by the change of the component M from K to Tl. This lack of variation is possible evidence of the similarity of the antiferromagnetic ground states of α-(BEDT-TTF)$_2$TlHg(SCN)$_4$ and α-(BEDT-TTF)$_2$KHg(SCN)$_4$.

The frequencies $\nu_{\rm res}(B)$ of modes A, L, N, X, and L' cannot be extrapolated to the value $\nu_{\rm res}(B\rightarrow 0)=0$. Figure 7 shows that modes A and N extrapolate back to finite threshold fields as the frequency tends to zero. Moreover, line L appears to originate from the same threshold field B_c as mode N at zero frequency (Fig. 7), strongly suggesting that modes L and N are related. At higher frequencies, it is evident that modes L and L' extrapolate to a similar frequency $\nu_0\approx 110$ GHz in the limit $B\rightarrow 0$ (Fig. 7). Together, these features indicate a common mechanism for lines L, L', and N.

The behavior of some of the features of Fig. 7 can be interpreted using existing models of AFMR.[2,3,36–38] Qualitatively, many of the data resemble the AFMR lines expected when an external magnetic field is applied parallel to the easy axis of a uniaxial antiferromagnet;[36–38] this type of magnetic order (with the easy axis perpendicular to the Q2D planes) has been proposed to explain the low-temperature magnetic susceptibility of α-(BEDT-TTF)$_2$KHg(SCN)$_4$.[39] In this interpretation, the characteristic frequency $\omega_0=2\pi\nu_0$ at $B=0$ is the AFMR frequency. The application of finite magnetic field causes the main AFMR mode to split into two components, ω_+ and ω_-, differing in the direction of precession of their magnetization vectors. The frequency ω_+ is expected to increase with magnetic field, whereas ω_- should decrease. In the experimental data (Fig. 7), lines L' and L thus appear to correspond to the AFMR modes ω_+ and ω_-, respectively. This identification is supported by the similarity of the shapes of lines L and L', both of which are ''triangular'' in appearance (Fig. 5). At some higher applied magnetic field, the antiferromagnet will undergo a spin flop,[2,3,36–38] at which point the frequency of the ω_- mode should go to zero. Inspection of Fig. 7 suggests that the spin flop corresponds to B_c. At fields above the spin flop, a further mode ω_1 should be observed, with a frequency which increases with increasing applied field and which extrapolates to zero at the spin flop field.[36–38] From Fig. 7 we conclude that the N line probably corresponds to the ω_1 mode.

Thus an analysis of the experimental data (Figs. 5–7) suggests that many of the small, sharp features in the experimental magnetoabsorption spectra are caused by AFMR. Such good qualitative agreement is perhaps surprising, given the fact that the magnetic order in α-(BEDT-TTF)$_2$TlHg(SCN)$_4$ and α-(BEDT-TTF)$_2$KHg(SCN)$_4$ is thought to be due to spin-density-wave formation,[18–23] whereas the theoretical treatment of AFMR is derived for a two-sublattice antiferromagnet[36–38] (see, however, Refs. 2 and 3, in which similar treatments are also applied successfully to spin-density-wave systems). Furthermore, even in the framework of the two-sublattice model, the identification of the resonant modes and hence the interpretation of the experimental data

depend strongly on the type of magnetic anisotropy. In general, the magnetic anisotropy may be intermediate between pure cases of uniaxial and easy-plane;[36] hence the corresponding mode structure may be different from the simple case which has been used to interpret the data in this work.

Finally, it must be noted that the presence of the AFMR-like lines *A* and *X* (Fig. 7) poses problems for the uniaxial interpretation, as modes with such behavior do not exist in such a scheme.[36–38] The easy-plane case[2,3,36–38] is even less helpful in this respect, as it cannot explain *any* of the lines observed in the experimental data. In particular the easy-plane scheme predicts the appearance of a major branch originating from the point $\omega=0$, $B=0$. Such a mode is not observed in the data.

In summary, many of the lines observed in the magnetoabsorption spectra possess the attributes of AFMR. However, a full interpretation of the apparent AFMR behavior of α-(BEDT-TTF)$_2$TlHg(SCN)$_4$ and α-(BEDT-TTF)$_2$KHg(SCN)$_4$ may require the development of models which take into account the band nature of the antiferromagnetic order in these materials. Such a model is beyond the scope of the present paper.

C. Electron-spin resonance

We now consider the structure of the magnetic resonance (line *S*) close to the predicted position of ESR (Fig. 5). ESR in α-(BEDT-TTF)$_2$KHg(SCN)$_4$ has been analyzed in detail using traditional resonant cavity techniques[5] to reveal that $g\approx 2.01$, and that the resonance is anomalously narrow at helium temperatures, with $\Delta B\sim 3\times 10^{-5}$ T.

In the present experiments, the external magnetic field and the high-frequency magnetic field were mutually perpendicular (Sec. II). Thus the selection rules for ESR were fulfilled, and so the appearance of an absorption around $g=2$ was expected. In Figs. 5 and 6, the vertical lines close to the *S* labels correspond to the calculated position of ESR with $g=2$. The data in Figs. 5 and 6 appear to indicate that, in the region $g\approx 2$, the width of the absorption line is much wider than that derived from ESR experiments carried out using a resonant cavity technique.[5] Moreover, in this region, a complex structure consisting of several close maxima arises in certain frequency ranges (Fig. 5). Note that a similarly broadened ESR line was observed in Ref. 4; in that case the organic conductor in question was very different from the BEDT-TTF salts, but the experimental configuration was very similar to that used in the present work.

The typical shape of the resonant magnetoabsorption in the vicinity of $g=2$ is shown in Fig. 8 on an enlarged field scale. To assist in the comparison of the data, the field axis is in units of $B\lambda$, where λ is the wavelength of the radiation; hence features corresponding to a constant g factor should occur at the same horizontal position. Figure 8 shows that the single ESR peak is absent, and in the region close to $g=2$ ($g=2$ is denoted by the vertical solid line) a characteristic ''double-peaked'' structure is observed. In the first accounts of this observation,[10] the complex line shape was interpreted as a superposition of the two close lines, one of which was assumed to be due to ESR of conduction electrons. However, neither of the two peaks occurs in the position expected from the g factor determined in ESR experiments.[5] Even if the interpretation of Ref. 10 is assumed to be valid (i.e., one of the lines *is* conduction-electron ESR), the nature of the other line remains obscure, as does the reason for the larger than expected width of both features (cf. Ref. 5).

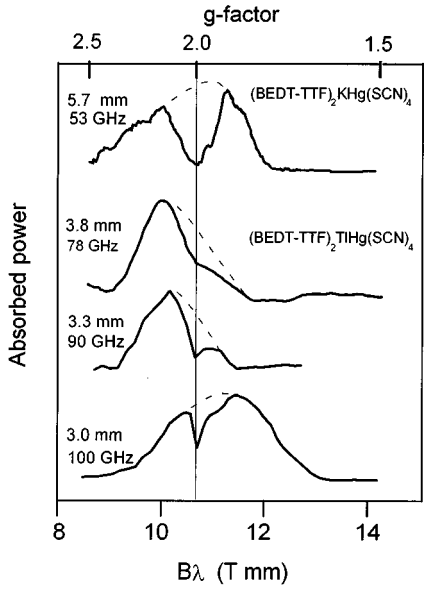

FIG. 8. Resonant absorption of millimeter wave radiation close to the predicted position of ESR ($T=1.8$ K). The upper curve shows data for α-(BEDT-TTF)$_2$KHg(SCN)$_4$, and the other curves data for α-(BEDT-TTF)$_2$TlHg(SCN)$_4$. To aid comparison, all data are plotted against reduced magnetic field. The figures near the curves correspond to the wavelength λ and frequency ν. The dashed line is a guide to the eye, and represents schematically the magnetoabsorption in the absence of the resonant transparency effect (see text for details).

Instead, we suggest that line *S* represents the superposition of a broad maximum and a narrow dip. The position of the dip corresponds within the experimental errors to $g=2$ (Fig. 8). In the theory of ''conventional'' metals, such structures are interpreted as the result of resonant transparency in thin metallic films undergoing ESR.[40] In this model, the broad maximum corresponds to ESR of conduction electrons, and the narrow dip is caused by resonant transparency due to the relatively slow damping of magnetic momentum inside the film.[40] The behavior predicted by the theory is in good qualitative agreement with the form of the data in Fig. 8. However, it is necessary to remark that in Ref. 40 the main reason for the slow damping is assumed to be the diffusion of electrons in the direction perpendicular to the metal surface. This type of motion is obviously more difficult in a Q2D organic metal than in the conventional case. However, the carriers do possess dispersion in the interplane direction (indeed, the magnetoresistance of BEDT-TTF salts can be measured with the current flowing in this direction[21]), so that the proposed mechanism is not unreasonable.

V. CONCLUSION

This paper has described a study of the magnetoabsorption of millimeter-wave radiation in the organic metals α-(BEDT-TTF)$_2$TlHg(SCN)$_4$ and α-(BEDT-TTF)$_2$KHg(SCN)$_4$ over the frequency range 30–120 GHz. The experimental magnetoabsorption data appear to display two distinct classes of spectral line. The largest features

(~10% of the signal) are interpreted as the cyclotron resonance of free 2D carriers. These resonances are characterized by broad linewidths ($\Delta B/B \sim 0.5-1$), and seem to be adequately described by the generalized Drude-Lorentz model. The observation of three features suggests the possible presence of three groups of 2D charge carriers. Furthermore, at least two of the corresponding cyclotron masses [$m_c \approx (0.5-0.8)m_0$, $m_c \approx (1-1.5)m_0$, and $m_c \approx 2.8m_0$] are frequency dependent, indicating the importance of many-body effects. At higher frequencies, two of the cyclotron masses tend toward the values observed in the far-infrared (i.e., submillimeter wavelength) experiments of Ref. 6.

The second type of resonance in the magnetoabsorption spectra appears as a series of narrow lines with fractional linewidths $\Delta B/B \sim 0.03-0.1$ and amplitudes 5–10 times smaller than those of the features interpreted as cyclotron resonance. The experimental data suggest that the collection of narrow lines results from the superposition of various antiferromagnetic resonance modes and the electron-spin resonance of conduction electrons. The presence of antiferromagnetic resonance is suggested by the observation of a line with a frequency which decreases with increasing magnetic field. The absorption interpreted as conduction-electron-spin resonance consists of the superposition of a narrow dip on a relatively broad maximum, possibly caused by resonant transparency of the type observed in thin metallic films.

The experimental data raise a number of questions. For example, the physical mechanisms that lead to frequency-dependent cyclotron masses are unclear, and the antiferromagnetic resonance model used to account for some of the narrow lines in the data certainly requires modification to be applicable to an antiferromagnet with a spin-density-wave ground state. Finally, a detailed identification of the three cyclotron resonance features must await a reliable model for the Fermi surfaces of α-(BEDT-TTF)$_2$TlHg(SCN)$_4$ and α-(BEDT-TTF)$_2$KHg(SCN)$_4$ in their antiferromagnetic ground states.

ACKNOWLEDGMENTS

This work was supported by INTAS programmes INTAS 93-2400 and INTAS 94-1788, and by EPSRC (UK) and the Royal Society (UK). Some aspects were also supported by the Programmes of the Russian Ministry of Science ''Fullerenes and atomic clusters'' and ''Microwaves.'' M.V. K. and A.E.K. acknowledge the partial financial support from the International Science Foundation, Grant No. RES300. The authors are very grateful to D. Shoenberg, B. A. Volkov, L. A. Falkovskii, S. A. Sharov, and A. A. Volkov for invaluable discussions.

[1] For a recent review, see Proceedings of the International Conference on Science and Technology of Synthetic Metals, Seoul, Korea, 1994, edited by Yung Woo Park and Hoo Fung Lee [Synth. Met. **69-71** (1994)].

[2] J. B. Torrance, H. J. Pedersen, and K. Bechgaard, Phys. Rev. Lett. **49**, 881 (1982).

[3] C. Coulon, R. Laversanne, J. Amiel, and P. Delhaes, J. Phys. C **19**, L753 (1986).

[4] M. Motokawa, L. Van Bockstal, and F. Herlach, J. Phys. C **18**, 5009 (1985).

[5] N. Kinoshita, M. Tokumoto, and H. Anzai, J. Phys. Soc. Jpn. **59**, 3410 (1990).

[6] J. Singleton, F. L. Pratt, M. Doporto, T. J. B. M. Janssen, M. Kurmoo, J. A. A. J. Perenboom, W. Hayes, and P. Day, Phys. Rev. Lett. **68**, 2500 (1992).

[7] S. Hill, A. Wittlin, J. van Bentum, J. Singleton, W. Hayes, J. A. A. J. Perenboom, M. Kurmoo, and P. Day, Synth. Met. **70**, 821 (1995).

[8] S. Hill, J. Singleton, F. L. Pratt, M. Doporto, W. Hayes, T. J. B. M. Janssen, J. A. A. J. Perenboom, M. Kurmoo, and P. Day, Synth. Met. **55-57**, 2566 (1993).

[9] J. Singleton, F. L. Pratt, M. Doporto, J. M. Caulfield, S. O. Hill, T. J. B. M. Janssen, I. Deckers, G. Pitsi, F. Herlach, W. Hayes, J. A. A. J. Perenboom, M. Kurmoo, and P. Day, Physica B **184**, 470 (1993).

[10] S. V. Demishev, N. E. Sluchanko, A. V. Semeno, and N. A. Samarin, Pis'ma Zh. Eksp. Teor. Fiz. **61**, 299 (1995) [JETP Lett. **61**, 313 (1995)].

[11] S. V. Demishev, A. V. Semeno, N. E. Sluchanko, N. A. Samarin, I. B. Voskoboinikov, V. V. Glushkov, A. E. Kovalev, and N. D. Kusch, Pis'ma Zh. Eksp. Teor. Fiz. **62**, 215 (1995) [JETP. Lett. **62**, 228 (1995)].

[12] O. Klein, S. Donovan, M. Dressel, and G. Gruner, Int. J. Infrared Millimeter Waves **14**, 2423 (1993).

[13] M. Dressel, O. Klein, G. Gruner, K. D. Carlson, H. H. Wang, and J. M. Williams, Phys. Rev. B **50**, 13 603 (1994).

[14] M. E. J. Boonman, S. O. Hill, A. Wittlin, J. A. A. J. Perenboom, J. S. Brooks, S. Uji, and R. Kato (unpublished).

[15] A. S. Perel, J. S. Brooks, C. J. G. M. Langerak, T. J. B. M. Janssen, J. Singleton, J. A. A. J. Perenboom, and L. Y. Chiang, Phys. Rev. Lett. **67**, 2072 (1991).

[16] L. P. Gor'kov and A. G. Lebed', Phys. Rev. Lett. **71**, 3874 (1993).

[17] M. Oshima, H. Mori, G. Saito, and K. Oshima, Chem. Lett. **1989**, 1159 (1989).

[18] M. V. Kartsovnik, A. E. Kovalev, and N. D. Kushch, J. Phys. (France) I **3**, 1187 (1993); M. V. Kartsovnik, H. Ito, T. Ishiguro, H. Mori, T. Mori, G. Saito, and S. Tanaka, J. Phys. Condens. Matter **6**, L479 (1994).

[19] J. S. Brooks, X. Chen, S. J. Klepper, S. Valfells, G. J. Athas, Y. Tanaka, T. Kinoshita, N. Kinoshita, M. Tokumoto, A. Anzai, and C. C. Agosta, Phys. Rev. B **52**, 14 457 (1995); S. Uji, T. Terashima, H. Aoki, J. S. Brooks, M. Tokumoto, N. Kinoshita, T. Kinoshita, Y. Tanaka, and H. Anzai, J. Phys. Condens. Matter **6**, L539 (1994); S. Uji, H. Aoki, J. S. Brooks, A. S. Perel, G. J. Athas, S. J. Klepper, C. C. Agosta, D. A. Howe, M. Tokumoto, N. Kinoshita, Y. Tanaka, and H. Anzai, Solid State Commun. **88**, 683 (1993).

[20] J. Caulfield, S. J. Blundell, M. S. L. du Croo de Jongh, P. T. J. Hendriks, J. Singleton, M. Doporto, F. L. Pratt, A. House, J. A. A. J. Perenboom, W. Hayes, M. Kurmoo, and P. Day, Phys. Rev. B **51**, 8325 (1995); N. Harrison, A. House, I. Deckers, J. Caulfield, J. Singleton, F. Herlach, W. Hayes, M. Kurmoo, and P. Day, Phys. Rev. B **52**, 5584 (1995).

[21] S. J. Blundell and J. Singleton, Phys. Rev. B **53**, 5609 (1996).

[22] T. Sasaki and N. Toyota, Phys. Rev. B **49**, 10 120 (1994); A. E. Kovalev, M. V. Kartsovnik, R. P. Shibaeva, L. P. Rozenberg, I. F. Schegolev, and N. D. Kushch, Solid State Commun. **89**, 575 (1994); M. V. Kartsovnik, A. E. Kovalev, R. P. Shibaeva, L. P. Rozenberg, and N. D. Kushch, Physica B **201**, 459 (1994).

[23] F. L. Pratt, T. Sasaki, N. Toyota, and H. Nagamine, Phys. Rev. Lett. **74**, 3892 (1995).

[24] *Strong and Ultrastrong Magnetic Fields and their Applications*, edited by F. Herlach, Topics in Applied Phys. Vol. 57 (Springer-Verlag, Berlin, 1985), p. 120.

[25] J. Caulfield, W. Lubczynski, F. L. Pratt, J. Singleton, D. Y. K. Ko, W. Hayes, M. Kurmoo, and P. Day, J. Phys. Condens. Matter **6**, 2911 (1994).

[26] See, e.g., M. Watts, R. J. Nicholas, J. J. Harris, and C. T. Foxon, in *Proceedings of the 20th International Conference on the Physics of Semiconductors*, edited by E. M. Anastassakis and J. D. Joannopoulos (World Scientific, Singapore, 1991), and references therein.

[27] D. Shoenberg, *Magnetic Oscillations in Metals* (Cambridge University Press, Cambridge, 1989); and (private communication).

[28] J. M. Williams, J. R. Ferraro, R. J. Thorn, K. D. Carlton, U. Geiser, H. H. Wang, A. M. Kini, and M. H. Whangbo, *Organic Superconductors (Including Fullerenes); Synthesis, Structure, Properties and Theory* (Prentice-Hall, Englewood Cliffs, NJ, 1989).

[29] A. A. Volkov, Yu. G. Goncharov, G. V. Kozlov, S. P. Lebedev, A. M. Prokhorov, Infrared Phys. **25**, 369 (1985).

[30] In order to check the hypothesis that some features of the magnetoabsorption are due to 2D carriers, experiments were carried out with the external magnetic field tilted with respect to the sample's conducting 2D planes. This geometry was obtained by rotating the bolometer with the sample. The repositioning of the bolometer leads to a new absorbed power baseline for the empty measuring unit, requiring the recalibration of the spectrometer for all the frequencies used. The time-consuming nature of this procedure is the reason why only a limited number of experiments were carried out with tilted samples.

[31] I. V. Lebedev, *Microwave Technology and Devices* (Vysshaya Shkola, Moscow 1970), Vol. 1, p. 181.

[32] M. Ya. Azbel' and E. A. Kaner, Zh. Eksp. Teor. Fiz. **32**, 896 (1956) [Sov. Phys. JETP **5**, 730 (1957)].

[33] T. Sasaki and N. Toyota, Solid State Commun. **75**, 93 (1990); N. D. Kushch, L. I. Buravov, M. V. Kartsovnik, V. N. Laukhin, S. I. Pesotskii, R. P. Shibaeva, L. P. Rozenberg, E. B. Yagubskii, and A. V. Zvarykina, Synth. Metals **46**, 271 (1992).

[34] L. Degiorgi, H. R. Ott, F. Hulliger, and M. B. Maple, in *Abstracts of the Second International Workshop on Low-Energy Electrodynamics in Solids (LEES 2)* (Trest, Czech Republic, 1995), p. 49; L. Degiorgi, H. R. Ott, and F. Hulliger, Phys. Rev. B **52**, 42 (1995).

[35] S. O. Hill, Ph.D. Thesis, Oxford University, 1995.

[36] F. Keffer and C. Kittel, Phys. Rev. **85**, 329 (1952).

[37] T. Nagamya and K. Yosida, Adv. Phys. **4**, 1 (1955).

[38] A. Gurevich and G. Melkov, *Magnetic Oscillations and Waves* (Nauka Moscow, 1994), p. 77.

[39] H. Mori, I. Hirabayshi, S. Tanaka, T. Mori, H. Inokuchi, K. Oshima, and G. Saito, Synth. Met. **55-57**, 2443 (1993); T. Sasaki, H. Sato, and N. Toyota, *ibid*. **41-43**, 2211 (1991).

[40] M. Ya. Azbel, V. I. Gerasimenko, and I. M. Lifshits, Zh. Eksp. Teor. Fiz. **32**, 1212 (1957) [Sov. Phys. JETP **5**, 986 (1957)].